**International Journal of Advanced Science and Research**
**ISSN: 2455-4227**
**Impact Factor: RJIF 5.12**
**www.allsciencejournal.com**
**Volume 2; Issue 6; November 2017; Page No. 33-41**

# Structural, magnetic and electrochemical properties of $Co_xZn_{1-x}Fe_2O_4$ nanoparticles synthesized by co-precipitation method

**K Sathiyamurthy, * P Sivagurunathan**
Department of Physics, Annamalai University, Annamalai Nagar, Tamil Nadu, India

**Abstract**
Cobalt zinc ferrite nanoparticles, $Co_xZn_{1-x}Fe_2O_4$(x=0.3, 0.5 and 0.7), have been prepared by the co-precipitation method and annealed at different temperatures. The structural and magnetic properties of the samples were determined and characterized by X-ray analysis showed that the samples were cubic spinel. Enhancement of crystallinity and particle size was observed with the increase in annealing temperatures. The increase in cobalt concentration in zinc ferrite nanoparticles resulted in the decrease of lattice parameter, unit cell volume and increase X-ray density were observed. Thermo gravimetric and differential thermal analysis (TG/DTA) method was used to confirm the formation of cobalt zinc ferrite nanoparticles. FTIR spectra confirm that the presence of metal oxide stretching vibration is attributed to the formation of cobalt zinc ferrite nanoparticles. The cobalt zinc ferrite nanoparticles annealed at 600 °C were characterized by using FESEM with EDAX, FETEM with SAED pattern. The surface morphology of cobalt zinc ferrite nanoparticles studied through FESEM and FETEM indicate that the particles were in spherical shape. EDAX analysis revealed the presence of Co, Zn, Fe and O content in cobalt zinc ferrite nanoparticles, and it's varied with the Co concentration. The M–H curve of cobalt zinc ferrite nanoparticles shows a ferromagnetic behavior at room temperature. The magnetic measurements showed that the saturation magnetization and coercivity increased with increasing the cobalt content in zinc ferrite nanoparticles, and it is suitable for magnetic devices. The electrochemical performance of the nickel zinc ferrite nanoparticles was investigated by CV analysis. The higher capacitance value 449 $Fg^{-1}$ was observed for the scanning rate 5$mVs^{-1}$for $Ni_{0.7}Zn_{0.3}Fe_2O_4$ reflecting the good quality of nickel zinc ferrite nanoparticles, and it was suitable for supercapacitor application.

**Keywords:** ferrite, cobalt zinc ferrite nanoparticles, magnetic property, super capacitor

## 1. Introduction
In the recent past, interest on synthesis of nanostructured magnetic materials has developed in various research areas due to their potential applications. As a result, many researchers show extreme interest in the synthesis of conventional materials at the nanoscale. Experimental conditions play a vital role in determining the shape, size and purity of the nanoparticles. Spinel ferrite is one of the most attractive magnetic nanoparticles used in various fields, such as magnetic resonance imaging, heat transfer devices, and high density magnetic storage devices [1, 3]. Supercapacitors and batteries are popular now electrochemical energy storage system in recent days. The batteries distribute high energy density and low power density whereas, conventional capacitors deliver high power density and low energy density. Supercapacitor is attractive because it can afford high power density, high rate capability, and long cycle life [4, 5]. These supercapacitors have plentiful potential applications such as power electronics, electric vehicles, sensor, and computer backup etc., [6]. Zinc ferrite nanoparticles added with cobalt modified the properties such as magnetic properties, high corrosion resistivity and chemical stability [7]. Zinc ferrite nanoparticles possess normal spinel structure, where all the $Zn^{2+}$ ions are occupied at a sites namely tetrahedral, and all the $Fe^{3+}$ ions are occupied at B sites namely octahedral [8]. $CoFe_2O_4$ nanoparticles is an inverse spinel structure, where $Co^{2+}$ ions are in the B sites namely tetrahedral and $Fe^{3+}$ ions are accommodated both the A and B sites namely tetrahedral and octahedral respectively [9]. Therefore, cobalt zinc mixed ferrite has attracted considerable attention due to their potential applications. In recent days, ferrite nanoparticles have been prepared by using various methods, such as hydrothermal treatment [10], micro emulsion [11], solvothermal [12], micro-wave sintering [13], ceramic technique [14], sol–gel synthesis [15], solid state reaction [16] and co-precipitation method [17]. Among the aforesaid methods, chemical co-precipitation method is a very resourceful, easy to handle and efficient method for the synthesis of ferrite nanoparticles [18].
It is interesting to study the different concentrations of cobalt in zinc ferrite nanoparticles annealed at different temperatures providing a useful result. An attempt has been made to synthesis of $Co_xZn_{1-x}Fe_2O_4$ (x = 0.3, 0.5 and 0.7) nanoparticles using chemical co-precipitation method. Prepared samples were annealed at different temperatures (400 °C, 600 °C and 800 °C) and its effect on structural, thermal, morphological, magnetic and electrochemical properties were investigated by XRD, TG/DTA, FTIR, FESEM, FETEM, VSM and CV measurements.

## 2. Experimental
Cobalt added zinc ferrite ($Co_xZn_{1-x}Fe_2O_4$) nanoparticles (x=0.3, 0.5 and 0.7) were synthesized by using a co-

precipitation method [19]. All the chemicals were purchased from Merck (AR grade) of 99% purity used for the present work without any further purification. For the successful synthesis of $Co_xZn_{1-x}Fe_2O_4$ nanoparticles, aqueous solutions of Fe $(NO_3)_3.9H_2O$, Zn $(NO_3)_2.6H_2O$, Co $(NO_3)_2.6H_2O$ were dissolved in 20 ml of de-ionized water separately. Then the citric acid ($C_6H_8O_7$) dissolved in de-ionized water and then added into nitrate solution drop by drop. Appropriate amount of sodium hydroxide (NaOH) precipitating agent was added to the nitrates solution in order to obtain the precipitate. After getting black brown color solution, the resultant solution was stirred continuously 120 minutes at 60 °C in 750 rpm. Obtained product was washed several times by acetone and de-ionized water, and then the precipitate was dried in hot air oven at 100 °C for 2 hrs. Further, the synthesized nanoparticles were annealed for 3 hrs at 400 °C, 600 °C and 800 °C respectively.

### 2.1 Characterization technique

The obtained materials were made to undergo XRD analysis, which was performed by a Philips X` pert Pro 3040/60 diffractometer with $CuK_\alpha$ (λ=1.54060Å) radiation. XRD pattern was recorded in the range of 20° to 80°. As a result of using the Joint Committee on Powder Diffraction Standards (JCPDS) database the phase identification of the prepared sample was found out. Average crystalline sizes of the samples have been calculated by Debye-Scherer's formula [20].

$$D=\frac{K\lambda}{\beta \cos\theta} \quad (1)$$

Where D is mean crystalline size, *K* is a dimensionless shape factor, with a value close to unity. The shape factor has a typical value of about 0.9, but varies with the actual shape of the crystallite, λ is wavelength of radiated X-ray (in Å), θ is represent Bragg diffraction angle (in radian) and β is full-width at half maximum subsequent to corrected for instrumental error. The TG/DTA analysis was carried out using NETZSCH - STA 449 F3 JUPITER. FTIR spectra were recorded using Perkin Elmer FTIR model 2000 spectrophotometer from 1000 to 400 $cm^{-1}$. FESEM with EDAX was recorded using ZEISS SUPRA 40 VP SEM. Shape of the particles with micro structural properties were examined by FETEM JEM 2100F. The selected area electron diffraction (SAED) patterns were confirmed by dispersing the sample beyond a carbon covered copper grid. Magnetic measurements were carried out with the Quantum Design lakeshore model 7407 Vibrating sample magnetometer (VSM) and parameters saturation magnetization ($M_s$) and coercive force ($H_c$) were evaluated. An electrochemical property of the nanoparticles was investigated by using the cyclic voltammetry (CV) instrument model CHI 660.

## 3 Results and discussion

### 3.1 Structural properties

The X-ray diffraction pattern of $Co_xZn_{(1-x)}Fe_2O_4$ (x=0.3, 0.5 and 0.7) nanoparticles annealed at different temperatures namely 400 °C, 600 °C and 800 °C are shown in Fig. 1(a, b and c).

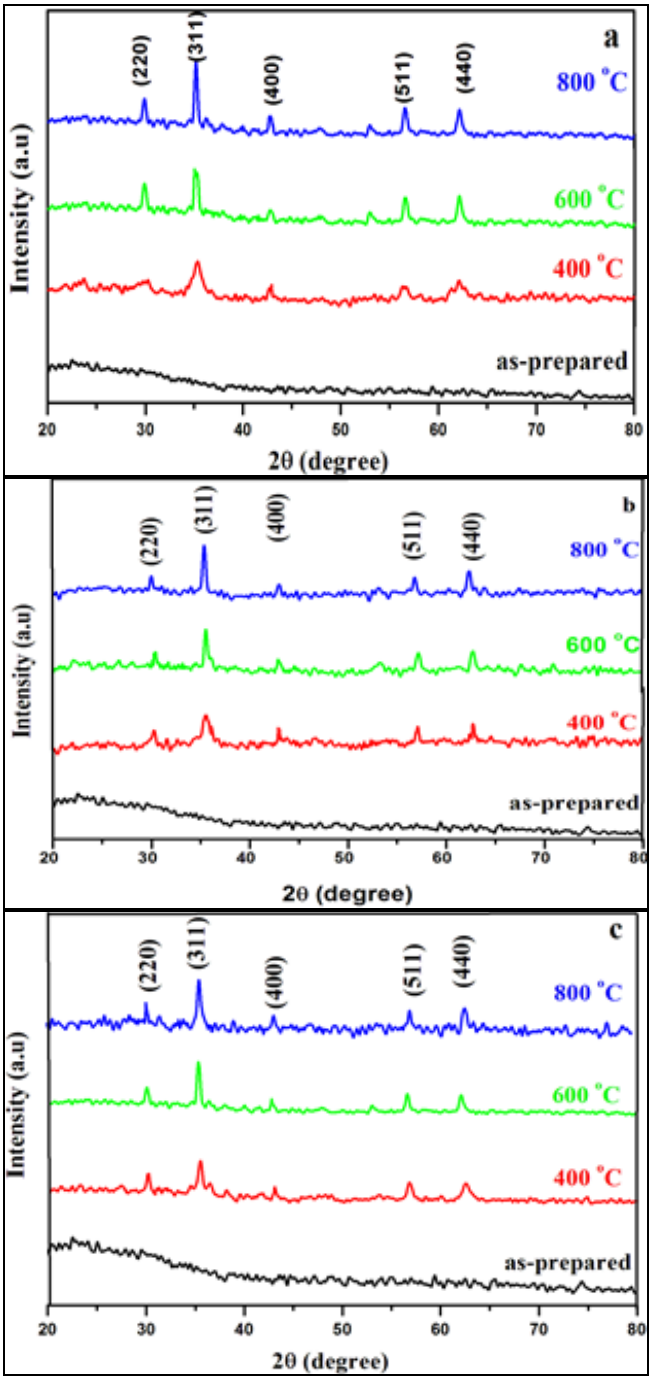


**Fig 1(a, b & c):** XRD Spectra of $Co_xZn_{(1-x)}Fe_2O_4$ (x=0.3, 0.5 and 0.7) nanoparticles as-prepared and annealed at different temperatures

As the prepared sample does not show any peaks which reveals that the prepared sample is amorphous in nature, so annealing process is essential and it has been carried out for further study. For that all synthesized samples were annealed at 400 °C, 600 °C and 800 °C and the XRD patterns of $Co_{0.3}Zn_{0.7}Fe_2O_4$, $Co_{0.5}Zn_{0.5}Fe_2O_4$ and $Co_{0.7}Zn_{0.3}Fe_2O_4$ nanoparticles having (220), (311), (400), (511) and (440) planes confirm that the synthesized nanoparticles possess a cubic spinel structure with Fd3m space group [21]. The peaks present in the obtained XRD patterns are well matched with JCPDS card no. 89-1012 ($ZnFe_2O_4$) and 22-1086 ($CoFe_2O_4$)

and it may suggest that the synthesized particles are cobalt zinc ferrite nanoparticles. Similar result was observed by Gozuak *et al.*, [22] for Synthesis and characterization of $Co_xZn_{1-x}Fe_2O_4$ magnetic nanoparticles. XRD analysis designate that the particle size increased with the increase of annealing temperatures reveals the growth of the nanoparticles is shown in Table 1.

**Table 1:** Particle size D (nm), Lattice parameter 'a' (Å), Unit cell volume (V) (Å) and X-ray density ($d_x$) of $Co_xZn_{(1-x)}Fe_2O_4$ (x=0.3, 0.5 and 0.7) nanoparticles annealed at different temperatures

| Material | Temperature °C | (D) (nm) | 'a' (Å) | (V) (Å) | $d_x$ (gm/cm$^3$) |
|---|---|---|---|---|---|
| $Co_{0.3}Zn_{0.7}Fe_2O_4$ | 400 °C | 10 | 8.453 | 603 | 4.14 |
| | 600 °C | 14 | 8.445 | 602 | 4.15 |
| | 800 °C | 18 | 8.425 | 598 | 4.18 |
| $Co_{0.5}Zn_{0.5}Fe_2O_4$ | 400 °C | 11 | 8.447 | 602 | 4.15 |
| | 600 °C | 17 | 8.439 | 600 | 4.16 |
| | 800 °C | 21 | 8.397 | 592 | 4.22 |
| $Co_{0.7}Zn_{0.3}Fe_2O_4$ | 400 °C | 13 | 8.420 | 597 | 4.18 |
| | 600 °C | 22 | 8.419 | 596 | 4.19 |
| | 800 °C | 26 | 8.376 | 587 | 4.24 |

The particle size of the $Co_{0.3}Zn_{0.7}Fe_2O_4$ at 400 °C, 600 °C and 800°C are 10, 14 and 18 nm respectively. The increases in particle size with annealing confirm the growth of cobalt zinc ferrite nanoparticles. Similar trend is noticed for $Co_{0.5}Zn_{0.5}Fe_2O_4$ and $Co_{0.7}Zn_{0.3}Fe_2O_4$ nanoparticles. The particle size of $Co_{0.3}Zn_{0.7}Fe_2O_4$, $Co_{0.5}Zn_{0.5}Fe_2O_4$ and $Co_{0.7}Zn_{0.3}Fe_2O_4$samples annealed at 400 °C are 10, 11 and 13 nm respectively. An identical result has been observed for the cobalt zinc ferrite nanoparticles annealed at 600 °C and 800 °C. The increasing particle size with increasing cobalt concentration is observed in the present study is close agreement with Mehran *et al.*, [23] for the synthesis of CoZn ferrite nanoparticles. This could be ascribed to the smaller covalent radius of Co cation (1.26 Å) than Zn cation (1.25 Å) [24]. Structural parameters such as, lattice parameter (a) of the annealed $Co_xZn_{(1-x)}Fe_2O_4$ (x=0.3, 0.5 and 0.7) nanoparticles have been calculated by using this relation is given by

$$a = d\sqrt{(h^2+k^2+l^2)} \quad (2)$$

Here, `a` is the lattice parameter, d is the interplanar spacing, and h, k, and l are the Miller indices of the crystal planes. The interplanar spacing d can be calculated by using the Bragg law of X-ray diffraction. The unit cell volume is calculated by using the following equation, which depends on the lattice Parameter.

$$\text{Volume of the unit cell } V=a^3 \text{ (Å)} \quad (3)$$

The lattice parameter and unit cell volume decreased with increasing the annealing temperatures of $Co_xZn_{(1-x)}Fe_2O_4$ (x=0.3, 0.5 and 0.7) nanoparticles are shown in Table 1. The decrease lattice parameter and unit cell volume with increase in Co concentration is observed in the present study suggest the configuration of a homogeneous solid solution [25].

The X-ray density ($d_x$) values are calculated from the XRD data using the relation is given by

$$d_x = ZM / Na^3 \quad (4)$$

Here, $d_x$ is the X-ray density (g/cm$^3$), Z is the number of molecules per unit cell (Z = 8 for spinel system), M is the molecular weight of the sample, N is the Avogadro's number, and 'a' is the lattice parameter. Table 1 indicates that the X-ray density ($d_x$) are increased with increasing annealed temperatures from 400 °C to 600 °C and 600 °C to 800 °C for a cobalt zinc ferrite nanoparticles. It is interesting to note that increasing X-ray density with increasing cobalt concentrations from $Co_{0.3}Zn_{0.7}Fe_2O_4$ to $Co_{0.5}Zn_{0.5}Fe_2O_4$ and $Co_{0.5}Zn_{0.5}Fe_2O_4$ to $Co_{0.7}Zn_{0.3}Fe_2O_4$ in all temperatures are observed. The X-ray density depends upon the lattice parameter and molecular weight of the sample. This is expected since the lighter cobalt ion replaces a heavier zinc ion, in addition to the decrease in lattice parameter [26].

### 3.2 TG/DTA

The TG/DTA curves of the dried precursor sample of $Co_{0.5}Zn_{0.5}Fe_2O_4$ nanoparticles from 35 °C to 850 °C are shown in Fig. 2.

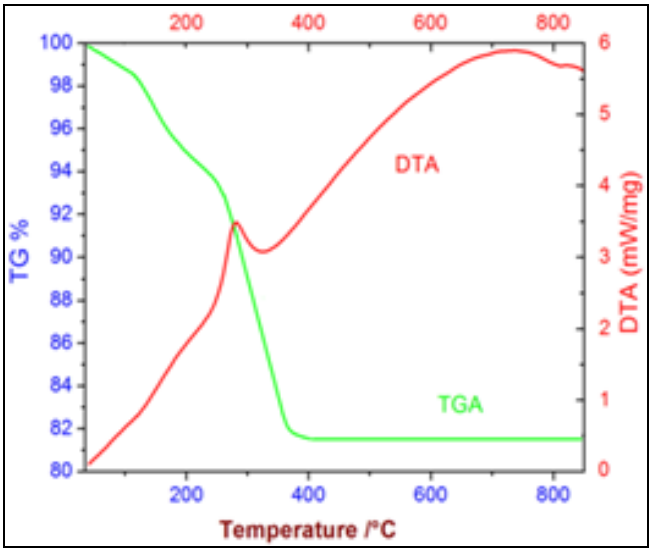


**Fig 2**: TG/DTA analysis of $Co_{0.5}Zn_{0.5}Fe_2O_4$ nanoparticles

The first stage of weight loss is observed in TGA curve at a temperature below 99 °C (2%) due to desorption of water vaporization of hydroxyl group. The second weight loss is observed in the range from 99 °C to 210 °C (6 %) as a result of decomposition of organic templates. The final weight loss of (7%) is observed in between 210 °C and 391 °C due to crystallization of the final product. No weight loss is observed beyond 391 °C indicating the formation of cobalt zinc ferrite nanoparticles. The TG curve shows that there is a continuous and gradual weight loss up to about 391 °C and no weight loss is recorded for further increasing of temperature [27]. The DTA curve shows the presence of one endothermic peak and one exothermic peak at 281 and 326 °C respectively. The endothermic peak come out due to loss of absorbed water and the exothermic peak at 326 °C is accompanied with the decomposition of the metal hydroxides [28].

### 3.3 Functional group analysis

FTIR spectra of $Co_xZn_{(1-x)}Fe_2O_4$ (x=0.3, 0.5 and 0.7) nanoparticles annealed at 400 °C, 600 °C and 800 °C have been obtained in the frequency range of 1000-400 $cm^{-1}$ is shown in Fig. 3(a, b and c).

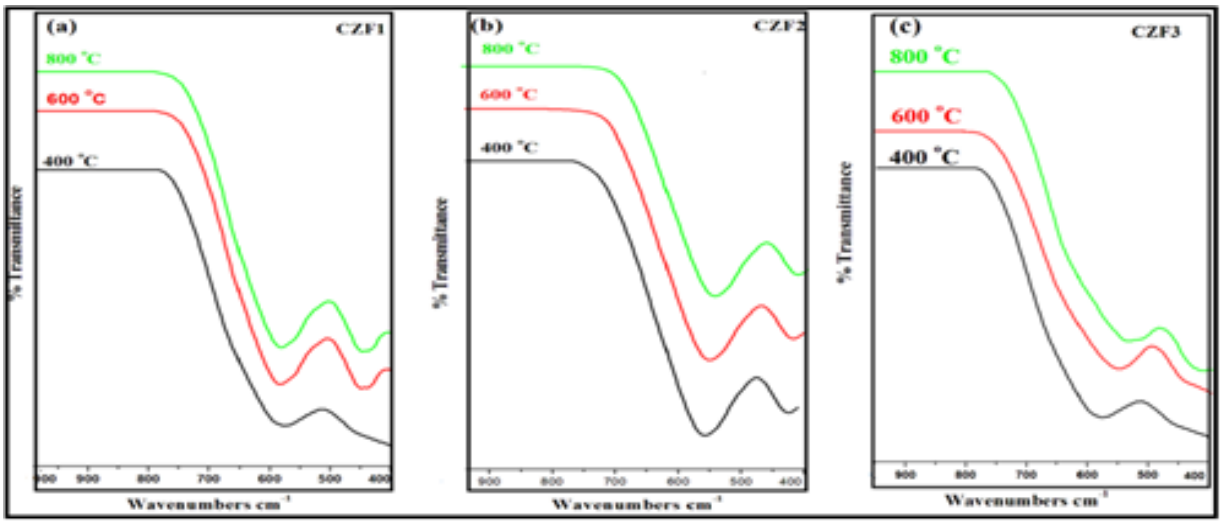


**Fig 3(a, b & c):** FTIR spectra of $Co_xZn_{(1-x)}Fe_2O_4$ (x=0.3, 0.5 and 0.7) nanoparticles annealed at different temperatures

There are two strong absorption bands are observed in the FTIR spectra of $Co_{0.3}Zn_{0.7}Fe_2O_4$, $Co_{0.5}Zn_{0.5}Fe_2O_4$ and $Co_{0.7}Zn_{0.3}Fe_2O_4$ samples. The higher absorption band $\nu_1$ has been observed in the range of 594-578 $cm^{-1}$ corresponds to intrinsic stretching vibration of the tetrahedral position of Co-O/Zn-O and lower absorption band is observed in the range of 420-464 $cm^{-1}$ is assigned due to octahedral position of Fe-O/Co-O stretching vibration of the ferrite nanoparticles [29, 30]. The absorption bands of $Co_xZn_{(1-x)}Fe_2O_4$ (x=0.3, 0.5 and 0.7) samples annealed at different temperatures are summarized in Table 2.

**Table 2:** FTIR spectra of $Co_xZn_{(1-x)}Fe_2O_4$ (x=0.3, 0.5 and 0.7) nanoparticles annealed at 400 °C, 600 °C, and 800 °C

| Temperature °C | 400 °C | | 600 °C | | 800 °C | |
|---|---|---|---|---|---|---|
| Samples | $\nu_1$ ($cm^{-1}$) | $\nu_2$ ($cm^{-1}$) | $\nu_1$ ($cm^{-1}$) | $\nu_2$ ($cm^{-1}$) | $\nu_1$ ($cm^{-1}$) | $\nu_2$ ($cm^{-1}$) |
| $Co_{0.3}Zn_{0.7}Fe_2O_4$ | 562 | 420 | 568 | 424 | 572 | 427 |
| $Co_{0.5}Zn_{0.5}Fe_2O_4$ | 572 | 424 | 574 | 428 | 579 | 430 |
| $Co_{0.7}Zn_{0.3}Fe_2O_4$ | 577 | 426 | 580 | 430 | 586 | 432 |

### 3.4 Field emission scanning electron microscope (FESEM) with EDAX

The morphology of $Co_xZn_{(1-x)}Fe_2O_4$ (x=0.3, 0.5 and 0.7) nanoparticles annealed at 600 °C have been studied by means of the FESEM image is shown in Fig.4(a, b and c).

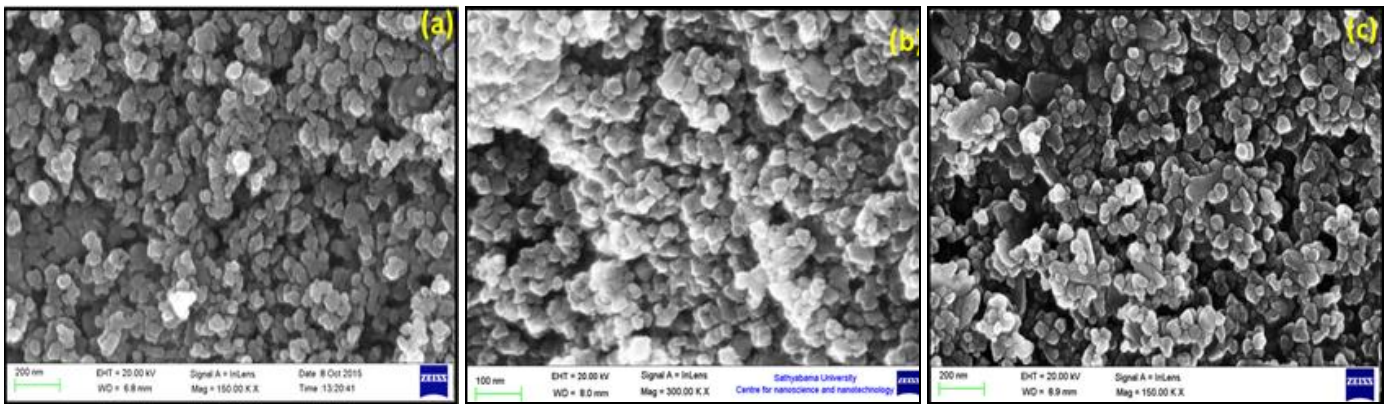


**Fig 4(a, b & c):** FESEM image of $Co_xZn_{(1-x)}Fe_2O_4$ (x=0.3, 0.5 and 0.7) nanoparticles annealed at 600 °C

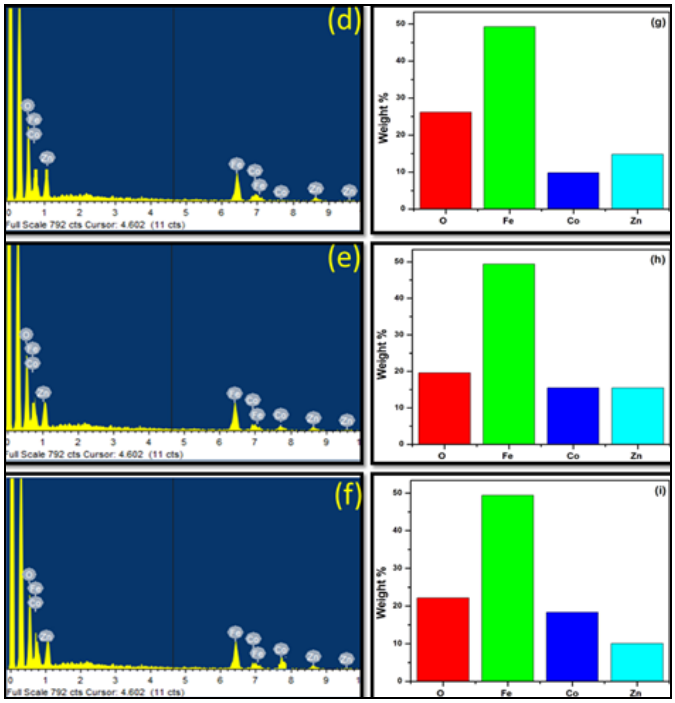


**Fig 4(d, e & f):** EDAX spectra of $Co_xZn_{(1-x)}Fe_2O_4$ (x=0.3, 0.5 and 0.7) nanoparticles annealed at 600 °C and (**g, h** and **i**) corresponding Quantitative results

The morphology can be able to identify the agglomeration in spherical nanoparticles, which is attributed due to the interaction between magnetic ferrite nanoparticles [31]. The EDAX spectrum of $Co_xZn_{(1-x)}Fe_2O_4$ (x=0.3, 0.5 and 0.7) nanoparticles annealed at 600 °C are shown in Fig.4 (d- f). From EDAX spectra of the elements present in the samples are identified as Co, Zn, Fe and O and it is shown in Fig.4 (d-f). The quantitative results of $Co_xZn_{(1-x)}Fe_2O_4$ (x=0.3, 0.5 and 0.7) nanoparticles annealed at 600 °C are shown in Fig.4 (g-i). It is seen from the figure shows that the weight and atomic percentage of the cobalt ions increased from $Co_{0.3}Zn_{0.7}Fe_2O_4$ to $Co_{0.5}Zn_{0.5}Fe_2O_4$ and $Co_{0.5}Zn_{0.5}Fe_2O_4$ to $Co_{0.7}Zn_{0.3}Fe_2O_4$, whereas the reverse trend is observed for zinc content confirm the $Co^{2+}$ ions replacing the $Zn^{2+}$ions. Similar result was observed by Anshu Sharma *et al.*, [32] for cobalt doped zinc ferrites nanoparticles using metallo-organic decomposition technique.

### 3.5 Field emission transmission electron microscope (FETEM) with SAED

FETEM images of $Co_xZn_{(1-x)}Fe_2O_4$ (x=0.3, 0.5 and 0.7) nanoparticles intend morphology is shown in Fig. 5(a, b and c).

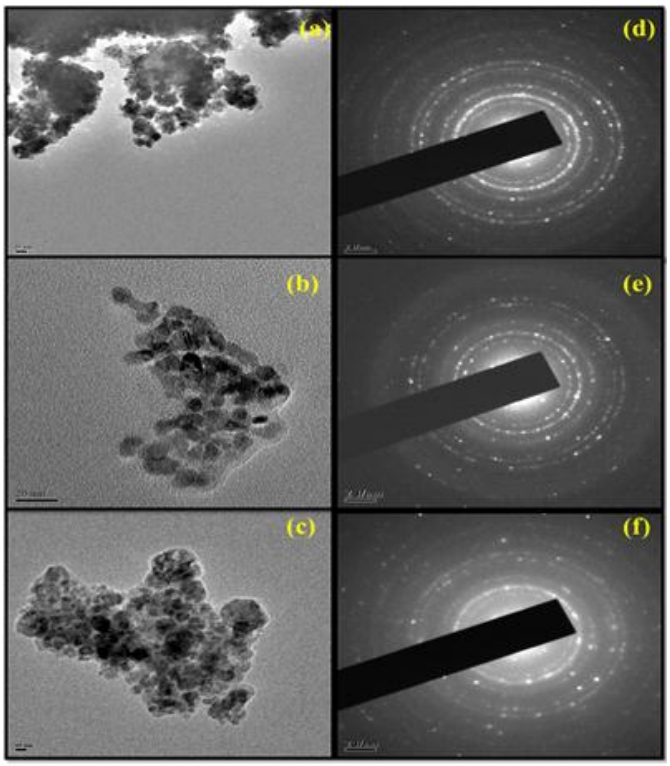


**Fig 5 (a, b & c):** FETEM image of $Co_xZn_{(1-x)}Fe_2O_4$ (x=0.3, 0.5 and 0.7) nanoparticles annealed at 600 °C and (d) (e), (f) resultant SAED.

The FETEM images of $Co_xZn_{(1-x)}Fe_2O_4$ (x=0.3, 0.5 and 0.7) nanoparticles annealed at 600 °C which confirms the particles are agglomerated with spherical shape [33]. From Fig. 5(a, b and c), the average particle size is found to be 14.2, 17.8 and 23.4 nm for the samples $Co_{0.3}Zn_{0.7}Fe_2O_4$, $Co_{0.5}Zn_{0.5}Fe_2O_4$ and $Co_{0.7}Zn_{0.3}Fe_2O_4$, respectively. This is well agree with those observation made by XRD. The resultant selected area electron diffraction pattern (SAED) of spherical shaped $Co_xZn_{(1-x)}Fe_2O_4$ (x=0.3, 0.5 and 0.7) is shown in Fig. 5(d, e and f). From the SAED pattern rings match well with standard powder diffraction information of spinel $CoFe_2O_4$ and $ZnFe_2O_4$ samples. The figure shows a SAED patterns reveals

the ordered structure of cobalt zinc ferrite nanoparticles which is in good agreement with XRD results showing the good crystalline nature of cobalt zinc ferrite nanoparticles [34].

### 3.6 Magnetic properties

The variation of magnetization ($M_s$) as a function of applied field ($H_c$) at room temperature for the samples $Co_xZn_{(1-x)}Fe_2O_4$ (x=0.3, 0.5 and 0.7) nanoparticles annealed at 600 °C shows a clear M-H curves as shown in Fig.6(a, b and c). The saturation magnetization ($M_s$) and coercivity ($H_c$) of $Co_xZn_{(1-x)}Fe_2O_4$ (x=0.3, 0.5 and 0.7) annealed at 600 °C are provided in Table 3.

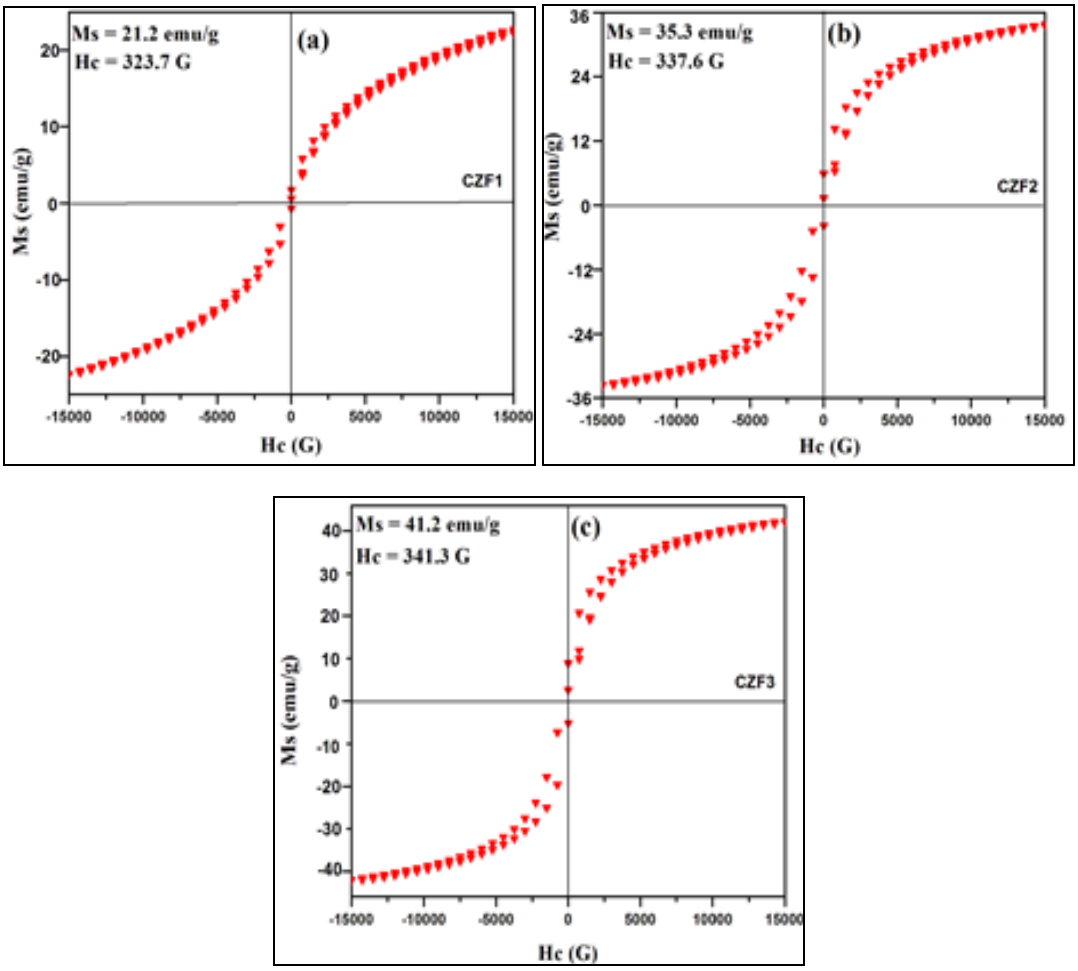


**Fig 6(a, b & c):** Room temperature M-H curves for $Co_xZn_{(1-x)}Fe_2O_4$ (x=0.3, 0.5 and 0.7) nanoparticles annealed at 600 °C

**Table 3:** Saturation magnetization ($M_s$) and Coercivity ($H_c$) value of $Co_xZn_{(1-x)}Fe_2O_4$ (x=0.3, 0.5 and 0.7) nanoparticles annealed at 600 °C

| Material | $M_s$ (emu/g) | $H_c$ (G) |
|---|---|---|
| $Co_{0.3}Zn_{0.7}Fe_2O_4$ | 21.2 | 323.7 |
| $Co_{0.5}Zn_{0.5}Fe_2O_4$ | 35.3 | 337.5 |
| $Co_{0.7}Zn_{0.3}Fe_2O_4$ | 41.2 | 341.3 |

The low field region of the magnetization increases with increasing applied magnetic field. It can be seen that all the magnetization curves are saturated at higher field region and the hysteresis curves for cobalt zinc ferrite nanoparticles resulting an S shaped hysteresis curve and suggesting the ferromagnetic behavior of the material at room temperature [35]. From Fig. 6, it is observed that $Co_{0.3}Zn_{0.7}Fe_2O_4$ obtained a saturation magnetization value of 21.2emu/g and the coercivity value of 323.7 G. While increasing the concentration of Co content $Co_{0.5}Zn_{0.5}Fe_2O_4$ and $Co_{0.7}Zn_{0.3}Fe_2O_4$, the values of both the saturation magnetization and the coercivity get increased. In a cubic structure of spinel ferrites, the magnetic order is mainly constructed due to super exchange interactions between metal ions of sub-lattices A and B sites. In $ZnFe_2O_4$, $Zn^{2+}$ preferably occupies the tetrahedral (A) sites and $Fe^{3+}$ prefers the octahedral sites (B). $CoFe_2O_4$ has an inverse spinel structure in which $Co^{2+}$ occupies B site and $Fe^{3+}$ ions equally taken A and B sites, with their spins in the opposite direction [36]. The magnetic moments of $Fe^{3+}$ are mutually compensated, and the resulting moment of the ferrite is due to the magnetic moments of bivalent cations $Co^{2+}$ in the B positions. Replacement of $Co^{2+}$ with $Zn^{2+}$ leads to introduction of non-magnetic $Zn^{2+}$ ions into A sites, thus increasing the saturation magnetization, $M_s$, leading to an increased magnetization [37].

### 3.7 Cyclic Voltammetry (CV)

The cyclic voltammetry study for $Co_xZn_{(1-x)}Fe_2O_4$ (x=0.3, 0.5 and 0.7) nanoparticles annealed at 600 °C electrode is carried out, and it is recorded at different scan rates 5, 10, 20, 30, 50, and 100 $mVs^{-1}$ shown in Fig.7 (a, b and c).

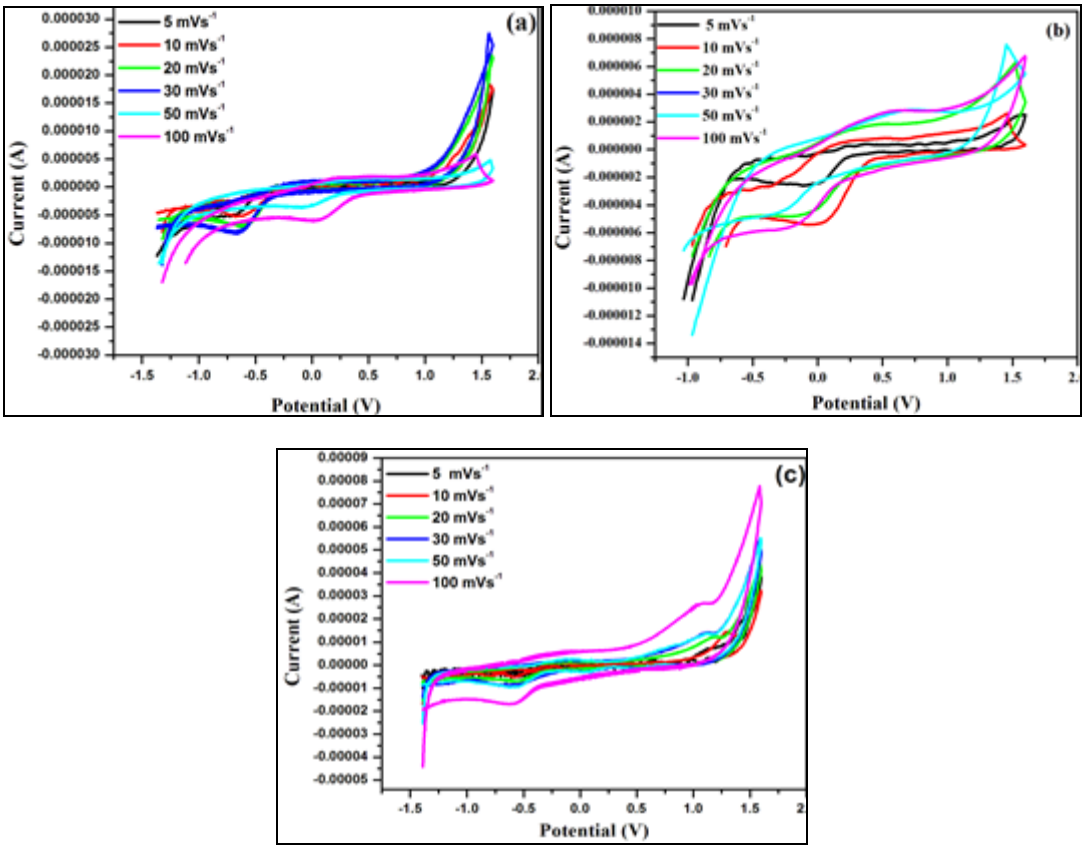


**Fig 7(a, b & c):** CV pattern of $Co_xZn_{(1-x)}Fe_2O_4$ (x=0.3, 0.5 and 0.7) nanoparticles annealed at 600 °C

Ideal rectangular shape is observed in the CV sure for 5 $mVs^{-1}$. The pseudo-capacitive nature is confirmed for the $Co_xZn_{(1-x)}Fe_2O_4$ (x=0.3, 0.5 and 0.7) samples annealed at 600 °C as the CV pattern changes with increasing scan rate. The specific capacitances ($C_S$) values of our desired synthesized material cobalt zinc ferrite electrode can be calculated using the relation [38].

$$Cs = \frac{Q}{\Delta v.m} \quad (5)$$

Here, Cs is the specific capacitance, Q signifies the anodic and cathodic charges on each scanning, m specifies the mass of the electrode material (mg) and Δv means the scan rate ($mVs^{-1}$) fixed in examining, tetra butyl ammonium perchlorate 0.2 M with a standard three electrode configuration consisting of a sample (working electrode), an Ag/AgCl (reference electrode) and a high platinum wire (counter electrode) is taken during electrochemical measurements [39]. Different scan rate starting from 5 $mVs^{-1}$ to 100 $mVs^{-1}$ is done and their equivalent specific capacitance value decreased as the scan rate increase which is illustrated in Table 4

**Table 4:** The specific capacitance of the $Co_xZn_{(1-x)}Fe_2O_4$ (x=0.3, 0.5 and 0.7) samples annealed at 600 °C for different scan rates

| Different Scan Rate ($mVs^{-1}$) | specific capacitance $Fg^{-1}$ | | |
|---|---|---|---|
| | $Co_{0.3}Zn_{0.7}Fe_2O_4$ | $Co_{0.5}Zn_{0.5}Fe_2O_4$ | $Co_{0.7}Zn_{0.3}Fe_2O_4$ |
| 5 | 300 | 344 | 376 |
| 10 | 186 | 220 | 272 |
| 20 | 74 | 96 | 98 |
| 30 | 42 | 55 | 57 |
| 50 | 21 | 25 | 29 |
| 100 | 3 | 7 | 9 |

A higher capacitance value of 376 $Fg^{-1}$ is recorded for $Co_{0.7}Zn_{0.3}Fe_2O_4$ samples than $Co_{0.3}Zn_{0.7}Fe_2O_4$ and $Co_{0.5}Zn_{0.5}Fe_2O_4$. The present study reveals that the better concentration as $Co_{0.7}Zn_{0.3}Fe_2O_4$ samples, exhibiting higher specific capacitance. Higher specific capacitance value at low scan rate has been detected in the present study i.e.,5 $mVs^{-1}$ propose that the ionic diffusion takes place in, both inner and outer surfaces depict lower specific capacitance values detected for higher scan rates specify that the ionic diffusion takes place only for outer surfaces [40]. The greater specific capacitance value detected in the present study confirms the better crystallinity of the $Co_{0.7}Zn_{0.3}Fe_2O_4$ nanoparticles, and it helps to attain a better super capacitor.

## 4. Conclusions

Cobalt zinc ferrite nanoparticles have been synthesized by

chemical co-precipitation method and annealed at 400 °C, 600 °C and 800 °C. Structural, compositional, magnetic and electrochemical behaviour of the annealed samples were well studied. Different synthesis parameters, which are found to be significant, have been optimized in order to get controlled size nanoparticles. XRD and FTIR study confirmed the composition and structure of synthesized spinel ferrite. An average crystallite size shows an increasing tendency for both annealing temperatures and increasing cobalt concentration. This was reflected with the variations of parameters such as lattice parameter, cell volume and X-ray density were observed in cobalt zinc ferrite nanoparticles. No weight loss was observed from 391 °C in TGA curve confirmed the formation of cobalt zinc ferrite nanoparticles. FESEM with EDAX and FETEM with SAED shows confirm the spherical morphology of synthesized nanoparticles. The magnetic properties such as coercivity and saturation magnetization were calculated from hysteresis loops. The enhanced magnetic properties at higher concentration of Co added in zinc ferrite nanoparticles were found to be suitable for magnetic devices. Higher capacitance value of 376 $Fg^{-1}$ $Co_{0.7}Zn_{0.3}Fe_2O_4$ is obtained for CV study suggesting that the synthesized nanoparticles could be suitable for super capacitance application.

## 5. Reference


1. Sousa MH, Tourinbo FA. New Electric Double-Layered Magnetic Fluids Based on Copper, Nickel, and Zinc Ferrite Nanostructures. J Phys Chem. B, 2000; 105:168.
2. Raj K, Moskowitz R, Casciari R. Advances in ferrofluid technology. J Magn Magn Mater, 1995; 149:174.
3. McMichael RD, Shull RD, Swartzendruber LJ, Bennett LH. Magnetocaloric effect in superparamagnets. J Magn Magn Mater, 1992; 111:29.
4. Chen D, Wang Q, Wang R, Shen G. Ternary oxide nanostructured materials for supercapacitors: a review. Journal of Materials Chemistry. 2015; 3(19):10158-10173.
5. Lavela P, Tirado JL. $CoFe_2O_4$ and $NiFe_2O_4$ synthesized by sol–gel procedures for their use as anode materials for Li ion batteries. Journal of power sources. 2007; 172(1):379-387.
6. Prasad KR, Miura N. Electrochemically synthesized $MnO^{2-}$based mixed oxides for high performance redox supercapacitors. Electrochemistry Communications. 2004; 6(10):1004-1008.
7. He HY. Magnetic properties of $Co_{0.5}Zn_{0.5}Fe_2O_4$ nanoparticles synthesized by a template-assisted hydrothermal method. J Nanotechnol. 2011.doi:10.1155/2011/182543
8. Vaidyanathan G, Sendhilnathan S, Arulmurugan R. Structural and magnetic properties of $Co_{1-x}Zn_xFe_2O_4$ nanoparticles by co-precipitation method. J Magn Magn Mater, 2007; 313:293-299.
9. Arumurugan R, Vaidyanathan G, Sendhilnathan S, Seyadevan B. Co–Zn ferrite nanoparticles for ferrofluid preparation: study on magnetic properties. Physica B, Condens Matter, 2005; 363:225.
10. Wei Wang, Ri Chen, Xiruo Zhao, Yajun Zhang, Jinliang Zhao, Feng Li. Synthesis and Characteristics of Superparamagnetic $Co_{0.6}Zn_{0.4}Fe_2O_4$ nanoparticles by a Modified Hydrothermal Method. J Am Ceram Soc. 2013; 96(7):2245–2251.
11. Sanjeev Kumar, Vaishali Singh, Saroj Aggarwal, Uttam Kumar Mandal, Kotnala RK. Monodisperse Co, Zn-Ferrite nanocrystals: Controlled synthesis, characterization and magnetic properties. J Magn Magn Mater. 2012; 324:3683-3689.
12. Zhigang Jian, Daping Ren, Qiuze Wang, Lixin Xu, Rongsun Zhu. Structural and magnetic properties of $Co_{1-x}Zn_xFe_2O_4$ nanorods prepared by the solvothermal annealing method. Ceramics International, 2013; 39:6113-6118.
13. Baykal A, Kasapoglu N, Koseoglu Y, Basaran AC, Kavas H, Toprak MS *et al.* Microwave-induced combustion synthesis and characterization of NixCo1− xFe2O4 nanocrystals (x= 0.0, 0.4, 0.6, 0.8, 1.0). Cent Eur J Chem., 2008; 6(1):125.
14. Hassadee A, Jutarosaga T, Onreabroy W. Effect of zinc substitution on structural and magnetic properties of cobalt ferrite. Procedia Engineering, 2012; 32:597-602.
15. Seung Wha Lee, Yeon Guk Ryu, Kea Joon Yang. Magnetic properties of $Zn^{2+}$ substituted ultrafine Co-ferrite grown by a sol-gel method. J Appl Phys., 2002; 91(1).
16. Patil VG, Shirsath SE, More SD, Shukla SJ, Jadhav KM. Effect of zinc substitution on structural and elastic properties of cobalt ferrite. J Alloys Compd., 2009; 488:199-203.
17. Dey S, Ghose J. Synthesis, characterisation and magnetic studies on nanocrystalline $Co_{0.2}Zn_{0.8}Fe_2O_4$. Materials Research Bulletin, 2003; 38:1653-1660.
18. Arulmurgun R, Vaidyanathan G, Sendhilnathan S, Jeyade-van B. Co-Zn ferrite nanoparticles for ferro-fluid preparation:study on magnetic properties. Physica B, Condens Matter., 2005; 363:225-231.
19. Ibrahim Sharifi H, Shokrollahi. Nanostructural, magnetic and Mossbauer studies of nanosized $Co_{1-x}Zn_xFe_2O_4$ synthesized by co-precipitation. J Magn Magn Mater., 2012; 324:2397-2403.
20. Hemeda M, El-Saadawy M. Effect of gamma irradiation on the structural properties and diffusion coefficient in Co-Zn ferrite. J Magn Magn Mater., 2003; 256:63.
21. Mozaffari M, Manouchehri S, Yousefi MH, Amighian J. The effect of solution temperature on crystallite size and magnetic properties of Zn substituted Co ferrite nanoparticles. J Magn Magn Mater., 2010; 322:383-388.
22. Gozuak F, Koseoglu Y, Baykal A, Kavas H. Synthesis and characterization of $Co_xZn_{1-x}Fe_2O_4$ magnetic nanoparticles via a PEG-assisted route. J Magn Magn Mater., 2009; 321:2170-2177.
23. Akther Hossaina AKM, Tabata H, Kawai T. Magnetoresistive properties of $Zn_{1-x}Co_xFe_2O_4$ ferrites. J. Magn. Magn. Mater, 2008; 320:1157-1162.
24. Mehran E, Shayesteh SF, Nasehnia F. Investigation of Structural and Magnetic Effects of Cobalt Doping in $ZnFe_2O_4$ Nanoparticles. Journal of Superconductivity and Novel Magnetism. 2016; 29(5):1241-1247.
25. Sonal S, Tsering N, Sandeep B, Kailash C. Effect of Zn substitution on the magnetic properties of cobalt ferrite

nanoparticles prepared via sol–gel route. J Electromagn Anal Appl., 2010; 2:376-381.
26. Huma Malik, Azhar Mahmood, Khalid Mahmooda, Maria Yousaf Lodhi, Muhammad Farooq Warsi, Imran Shakir, Hassan Wahabe, Asghar M, Muhammad Azhar Khana. Influence of cobalt substitution on the magnetic properties of zinc nanocrystals synthesized via micro-emulsion route. Ceramics International, 2014; 40:9439-9444.
27. Aghav PS, Dhage VN, Mane ML, Shengule DR, Dorik RG, Jadhav KM *et al.* Effect of aluminum substitution on the structural and magnetic properties of cobalt ferrite synthesized by sol–gel auto combustion process. Phys.B: Condens. Matter, 2011; 406:4350-4354.
28. Gonsalves LR, Mojumdar SC, Verenkar VMS. Synthesis and characterization of $Co_{0.8}Zn_{0.2}Fe_2O_4$ nanoparticles. J Therm Anal Calorim., 2011; 104:869-873.
29. Javed Iqba, Mubasher Rajpoot, Tariq Jan, Ishaq Ahmad. Annealing Induced Enhancement in Magnetic Properties of $Co_{0.5}$ $Zn_{0.5}$ $Fe_2$ $O_4$ nanoparticles. J Supercond Nov Magn., 2014; 27:1743-1749.
30. Tamara Slatineanua, Alexandra Raluca Iordana, Victor Oanceaa, Mircea Nicolae Palamarua, Ioan Dumitrub, Cristin Petrica Constantinb, Ovidiu Florin Caltun. Magnetic and dielectric properties of Co–Zn ferrite, Materials Science and Engineering B, 2013; 178:1040-1047.
31. Cornelia Muntean, Marius Bozdog, Sebastian Duma, Mircea Stefanescu. Study on the formation of $Co_{1-2x}Zn_xFe_2O_4$ system using two low-temperature synthesis methods. J Therm Anal Calorim. 2016; 123(1):117-126.
32. Manikandan A, John Kennedy L, Bououdina M, Judith Vijaya J. Synthesis, optical and magnetic properties of pure and Co-doped $ZnFe_2O_4$ nanoparticles by microwave combustion method. J Magn Magn Mater., 2014; 349:249-258.
33. Anshu Sharma, Kusum Parmar, Kotnala RK, Negi NS. Magnetic and dielectric properties of $Co_xZn_{1-x}Fe_2O_4$ synthesized by metallo-organic decomposition technique, IJAET. 2012; 5(1):544-554.
34. Nikam DS, Jadhav SV, Khot VM, Bohara RA, Hong CK, Mali SS, Pawar SH. Cation distribution, structural, morphological and magnetic properties of $Co_{1-x}Zn_xFe_2O_4$ x= 0-1 nanoparticles. RSC Advances. 2015; 5(3):2338-2345.
35. Gangatharan Sathishkumar, Chidambaram Venkataraju, Kandasamy Sivakumar. Synthesis, Structural and Dielectric Studies of Nickel Substituted Cobalt-Zinc Ferrite, Materials Sciences and Applications, 2010; 1:19-24.
36. He HY. Microstructural and magnetic property of $Co_{1-x}Zn_xFe_2O_4$ nanoparticles synthesized by the hydrothermal method. J Ceramic Processing Research. 2015; 16(3):313~318.
37. Eltabey MM, Aboulfotoh Ali N. Effect of Annealing Temperature on Structural and Magnetic Properties of Co-Zn Ferrite nanoparticles. International J Advanced Research. 2014; 2(6):184-192.
38. Gibin SR. Sivagurunathan P. Synthesis and characterization of nickel cobalt ferrite $Ni_{1-x}Co_xFe_2O_4$ nanoparticles by co-precipitation method with citrate as chelating agent. Journal of Materials Science: Materials in Electronics. 2017; 28(2):1985-1996.
39. Sathishkumar K, Shanmugam N, Kannadasan N, Cholan S, Viruthagiri G. Opto, magnetic and electrochemical characterization of $Ni_{1-x}Co_xO$ nanocrystals. Journal of Materials Science: Materials in Electronics. 2015; 26(3):1881-1889.
40. Pang SC, Wee BH, Chin SF. The capacitive behaviors of manganese dioxide thin-film electrochemical capacitor prototypes. International Journal of Electrochemistry, 2011.doi.org/10.4061/2011/397685.